

Geophysical Research Letters*



RESEARCH LETTER

10.1029/2023GL103591

Key Points:

- Group 1 alkenones are reliable indicators of cold-season temperatures
- Pre-industrial cold-season warmth between 1750 and 1850 CE in northeastern China
- Relatively warm cold season may be related to positive cold-season Arctic Oscillation conditions

Supporting Information:

Supporting Information may be found in the online version of this article.

Correspondence to:

Y. Yao, yaoyuan@xjtu.edu.cn

Citation:

Yao, Y., Wang, L., Huang, Y., Liang, J., Vachula, R. S., Cai, Y., & Cheng, H. (2023). Pre-industrial (1750–1850 CE) cold season warmth in northeastern China. *Geophysical Research Letters*, 50, e2023GL103591. https://doi.org/10.1029/2023GL103591

Received 7 MAR 2023 Accepted 11 MAY 2023

Author Contributions:

Conceptualization: Yuan Yao

Funding acquisition: Yuan Yao, Yanjun Cai, Hai Cheng
Investigation: Yuan Yao, Lu Wang
Methodology: Yuan Yao, Lu Wang
Software: Jie Liang
Supervision: Yuan Yao
Writing – original draft: Yuan Yao
Writing – review & editing: Yongsong
Huang, Jie Liang, Richard S. Vachula,
Yanjun Cai, Hai Cheng

Formal analysis: Yuan Yao, Lu Wang

© 2023. The Authors.

This is an open access article under the terms of the Creative Commons Attribution-NonCommercial-NoDerivs License, which permits use and distribution in any medium, provided the original work is properly cited, the use is non-commercial and no modifications or adaptations are made.

Pre-Industrial (1750–1850 CE) Cold Season Warmth in Northeastern China

Yuan Yao¹, Lu Wang¹, Yongsong Huang², Jie Liang³, Richard S. Vachula⁴, Yanjun Cai¹, and Hai Cheng¹

¹Institute of Global Environmental Change, Xi'an Jiaotong University, Xi'an, China, ²Department of Earth, Environmental and Planetary Sciences, Brown University, Providence, RI, USA, ³State Key Laboratory of Tibetan Plateau Earth System, Environment and Resources, Institute of Tibetan Plateau Research, Chinese Academy of Sciences, Beijing, China, ⁴Department of Geosciences, Auburn University, Auburn, AL, USA

Abstract Contrary to global warming projections, northern mid-latitude continents have suffered from an increased frequency of unusually cold winters during the last few decades. However, a lack of longer-term cold-season temperature records from mid-latitudes hampers our understanding of the forcing mechanisms of this temperature variability. Here we report a Group 1 alkenone-based high-resolution record of cold-season temperatures extending to the pre-industrial era (since 1700 CE) from Lake Luming in northeastern China. By comparing with the instrumental and historical records in the region, we verify the high efficacy of Group 1 alkenones as recorders of cold-season temperature variability. Our record shows pre-industrial warmth between 1750 and 1850 CE relative to anthropogenic industrial period (since 1850 CE), which is largely driven by variability of the Arctic Oscillation, with a negligible contribution from anthropogenic greenhouse-gas forcing. Our results highlight the importance of internal atmospheric circulation in driving cold-season temperatures in northeastern China.

Plain Language Summary Frequent occurrence of extreme cold events in northern mid-latitudes during the last few decades imposes significant social and economic impacts. Past reconstructions of longer-term cold-season temperature variability are of crucial importance for understanding past and future cold anomalies. Here we use a paleothermometer proxy based on Group 1 alkenone lipid biomarkers to reconstruct cold-season temperature variability of the last ~300 years from a freshwater lake in northeastern China. Our cold-season reconstruction is confirmed by the instrumental and historical records in the region. We show a relatively warm cold-season climate during the pre-industrial period of 1750–1850 CE relative to the period since the industrial revolution (since 1850 CE). More positive cold-season Arctic Oscillation (AO) conditions, rather than anthropogenic greenhouse-gas forcing, may explain this warmth, which is associated with the AO-induced reduction of cold air outbreaks over northeastern China. Our study suggests that internal atmospheric circulation has played an important role in driving cold-season temperature variability in northeastern China on our study timescales.

1. Introduction

Global mean annual temperatures have shown an accelerated warming trend in the last few decades in response to increasing anthropogenic forcing (Stocker et al., 2013), particularly in the Arctic (Pithan & Mauritsen, 2014). In cold seasons (winter and spring), however, land temperatures for large areas of northern mid-latitudes have experienced almost no warming or cooling trends during the same period (especially 1990–2013; J. Cohen et al., 2020) with frequent cold extremes, which is in sharp contrast to amplified Arctic warming (e.g., J. Cohen et al., 2020; J. L.Cohen et al., 2012; McCusker et al., 2016; Mori et al., 2019). This divergence of cold-season temperatures is known as the "warm Arctic-cold continents" pattern (Overland et al., 2011), but the underlying mechanisms remain incompletely understood. Cold-season temperature reconstructions of the mid-latitudes on timescales extending to the pre-industrial era can provide a critical natural context and long-term perspective for recent climate excursions, which are of crucial importance for understanding these climate dynamics.

Unfortunately, the vast majority of existing temperature proxies from various geological archives (e.g., lake and marine sediments, speleothems, tree rings, and ice cores) are strongly biased toward warm season or mean annual temperatures (e.g., PAGES 2k Consortium, 2017). Oxygen isotopic records from Arctic ice wedges

YAO ET AL. 1 of 10

19448007, 2023, 10, Downloaded from https://agupubs.onlinelibrary.wiley.com/doi/10.1029/2023GL103591 by Brown University Library, Wiley Online Library on [03/09/2023]. See the Terms

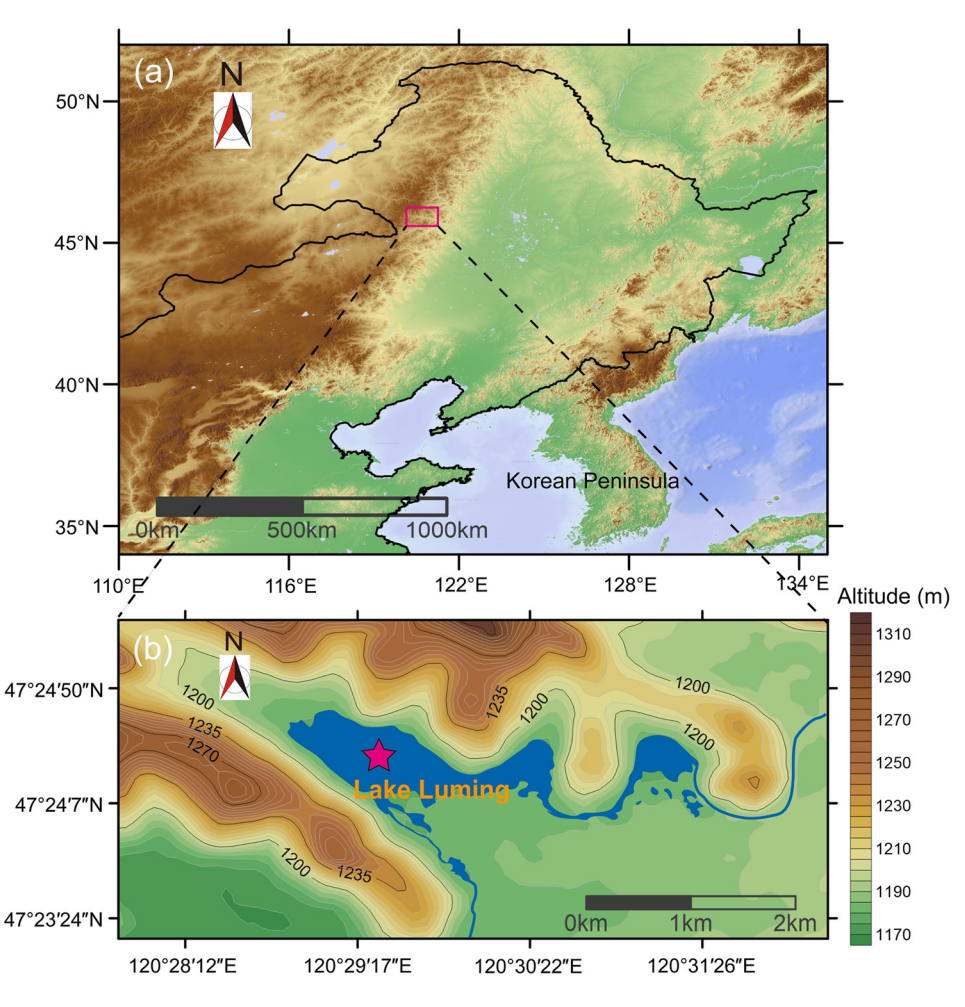


Figure 1. Map of study site. (a) Topographic map includes northeastern China and the location of the study site. (b) Contour map shows the location of the sediment core (red star) collected from Lake Luming and the lake's hydrological context.

(Holland et al., 2020; Meyer et al., 2015), stalagmites of the southern Ural Mountains (Baker et al., 2017), and peat α -cellulose of the southern Altai Mountains (Rao et al., 2020) have recently been interpreted as cold-season temperature signals for Holocene temperature reconstructions. However, these reconstructions are restricted to certain high-latitude regions (Baker et al., 2017; Holland et al., 2020; Meyer et al., 2015) or unique areas with snow/ice meltwater as a dominant water source (Rao et al., 2020). The distinctive long-chain alkenones (LCAs) produced by phylogenetically classified Group 1 Isochrysidales in freshwater lakes are powerful new tools for cold-season temperature reconstructions (Longo et al., 2018, 2020; Richter et al., 2021; Yao et al., 2019). The widespread occurrence of Group 1 LCAs in oligotrophic freshwater lakes throughout the northern mid- and high-latitudes (Longo et al., 2018; Yao et al., 2019) provides a valuable opportunity to address the knowledge gap regarding cold-season temperature variability in mid-latitude regions.

Here we present a ~ 300 years long, high-resolution record of cold-season temperature from volcanic Lake Luming in northeastern China ($\sim 40-54^{\circ}$ N; Figure 1) based on the unsaturation index (U_{37}^{K}) of Group 1 LCAs. Our study lake has high sediment accumulation rates with an average of ~ 0.27 cm/yr (Figure 2a), allowing for direct comparison with modern instrumental temperature data to verify proxy reliability. We compare our record with a series of potential forcing factors, including the Arctic Oscillation (AO), the North Atlantic Oscillation (NAO), greenhouse gas, solar irradiance, and volcanic aerosol forcings. Our data and analyses provide new insights into the underlying forcing mechanisms of cold-season temperature variability during the last ~ 300 years in northeastern China.

YAO ET AL. 2 of 10

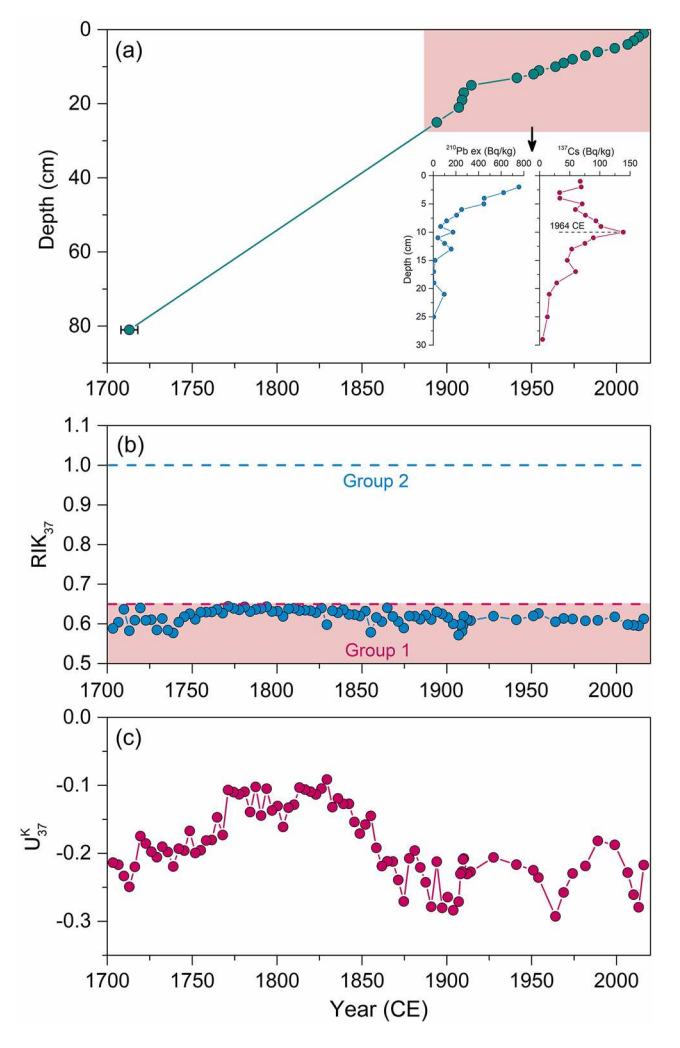


Figure 2. (a) Age model for the Lake Luming sediment core and downcore variations in (b) RIK₃₇ and (c) U_{37}^K values. Red shaded area in (b) represents the RIK₃₇ range of 0.5–0.65, indicating dominant Group 1 Isochrysidales.

2. Materials and Methods

2.1. Study Site

Lake Luming ($47^{\circ}24'-47^{\circ}25'N$, $120^{\circ}29'-120^{\circ}31'E$; 1,179 m a.s.l; Figure 1b), located in the Arxan-Chaihe volcanic field of the Greater Khingan Mountains in northeastern China, is a freshwater volcanically dammed lake (salinity measured on July 2016 CE was $\sim 0.02\%$; Yao et al., 2019). The lake formed due to the lava flows from Yanshan occurring in the Late Holocene (Wang et al., 2014), which blocks the Haraha River. The Haraha River flows through the lake from the southwest to the southeast. Lake Luming has a surface area of $\sim 1.59 \text{ km}^2$ and the maximum water depth is ~ 5 m (Yao et al., 2019). The regional mean annual air temperature is $\sim 2.55^{\circ}C$, and the mean annual precipitation is ~ 441 mm (1953–2021; from nearby Arxan weather station), with maximum and minimum precipitation in summer and winter, respectively.

2.2. Sampling and Chronology

We collected an 85-cm sediment core ($47^{\circ}24.4'N$, $120^{\circ}29.4'E$; LMH17) from Lake Luming from a water depth of \sim 3 m in July 2017 CE (Figure 1b). The core was subsampled at 1 cm intervals, and all samples were frozen at -20° C in the laboratory prior to analysis.

The chronology of the core has been well established by $^{137}\text{Cs}\text{-}^{210}\text{Pb}$ dating and a ^{14}C model (Lu et al., 2021). The ^{137}Cs activity peak was detected at 10 cm depth, which corresponds to 1964 CE (Appleby, 2002). The age model of our high-resolution sediment core above 25 cm depth (since 1894 CE) was constructed using a constant-rate-of-supply (CRS) model (Sanchez-Cabeza & Ruiz-Fernández, 2012) based on ^{210}Pb and using the ^{137}Cs peak as a fixed 1964 CE time marker (Figure 2a; the top 1 cm of core was assumed to date to 2016 CE). From 1700 CE (85 cm) to 1894 CE (25 cm), the chronology was established by linear interpolation to a ^{14}C age (1713 \pm 5 CE) of terrestrial plant fragments at 81 cm depth (Figure 2a).

2.3. Alkenone Analysis

All sediment samples were freeze-dried and extracted by sonication (3×) with dichloromethane (DCM)/methanol (MeOH) (9:1, v/v). Total lipid extracts

were purified by column chromatography with silica gel using the following sequence of eluents: n-hexane, DCM, and MeOH. The DCM fractions containing LCAs were further purified using column chromatography with silver nitrate-impregnated silica gel (\sim 10 weight %, +230 mesh from ALDRICH) with DCM and ethyl acetate (Novak et al., 2022). Following the method reported by Zheng et al. (2017), LCAs in the ethyl acetate fractions were analyzed using an Agilent 8890 gas chromatography (GC) system equipped with a flame ionization detector (FID) and a Restek Rtx-200 GC column (105 m \times 250 μ m \times 0.25 μ m) at Xi'an Jiaotong University, China. The following GC oven program was used: initial temperature of 50°C (hold 2 min), ramp 20°C/min–255°C, ramp 3°C/min–312°C (hold 35 min). Helium was used as the carrier gas and was held at a constant flow rate of 1.3 mL/min. The well-defined LCA profile from our previously reported Lake Wudalianchi samples (Yao et al., 2019) was used as a standard for the comparison of LCA peaks.

The alkenone unsaturation index U_{37}^K (Brassell et al., 1986), $U_{37}^{K'}$ (Prahl & Wakeham, 1987), and alkenone isomer-based RIK₃₇ (Longo et al., 2016) were calculated as follows:

$$U_{37}^{K} = \frac{C_{37:2} - C_{37:4}}{C_{37:2} + C_{37:3} + C_{37:4}}$$
 (1)

$$U_{37}^{K'} = \frac{C_{37:2}}{C_{37:2} + C_{37:3}}$$
 (2)

YAO ET AL. 3 of 10

$$RIK_{37} = \frac{C_{37:3a}}{C_{37:3a} + C_{37:3b}}$$
(3)

where the "a" and "b" subscripts refer to the $\Delta^{7,14,21}$ and $\Delta^{14,21,28}$ tri-unsaturated LCAs, respectively.

2.4. Statistical Analyses

We used wavelet coherence analysis (Torrence & Compo, 1998) to explore the potential impacts of total solar irradiance (TSI) and volcanic aerosol forcings on our U_{37}^K record on different timescales. The data used in the analyses were interpolated at 5 years time steps using the *interp. data set* function and a spline method in R. The statistical analyses were performed using the R biwavelet package (Grinsted et al., 2004).

3. Results and Discussion

3.1. Group 1 Alkenones in the Lake Luming Sediment Core

In lacustrine environments, alkenone-producing Isochrysidales are composed of two phylogenetically distinct groups: Group 1 and Group 2 (Theroux et al., 2010), with Group 1 occurring in freshwater/oligohaline lakes and Group 2 in brackish/saline lakes (Longo et al., 2016, 2018; Yao et al., 2019, 2022). Group 1 LCAs feature a highly specific profile with the presence of C_{38} Me ("Me" refers to methyl ketone) and two tri-unsaturated isomers $C_{37:3b}$ and $C_{38:3b}$ Et ("Et" refers to ethyl ketone) with $\Delta^{14,21,28}$ double bond positions (Longo et al., 2013, 2016; Yao et al., 2019). In particular, two tri-unsaturated isomeric C_{37} alkenones ($C_{37:3a}$ and $C_{37:3b}$) in LCA profiles produced by Group 1 Isochrysidales have similar abundances. Thus, the RIK $_{37}$ index based on the ratio of $C_{37:3a}$ and $C_{37:3b}$ isomers (Equation 3) can be used to evaluate the relative contributions of alkenones produced by Group 1 Isochrysidales in lake sediments (Longo et al., 2016, 2018; Yao et al., 2020). RIK $_{37}$ values of \sim 0.48–0.63 indicate that alkenones are produced primarily by Group 1 Isochrysidales (Longo et al., 2016, 2018; Yao et al., 2019).

We have previously confirmed that surface sediments from Lake Luming contain only Group 1 LCAs using a combination of organic geochemical and genomic analyses (Yao et al., 2019). In our sediment core from Lake Luming, LCA distributions display the typical characteristics of Group 1-type alkenones, with the presence of $C_{37:3b}$, $C_{38:3b}$ Et, and C_{38} Me (Figure S1 in Supporting Information S1). The RIK₃₇ values vary between 0.57 and 0.64 (Figure 2b), indicating that the LCAs are derived primarily from Group 1 Isochrysidales production throughout our sediment core. Therefore, our U_{37}^{K} paleotemperature record mainly reflects the temperature signal from the Group 1 growth season (Figure 2c).

3.2. Cold-Season Temperature Reconstruction Based on Group 1 Alkenones

The seasonal bloom timing of Group 1 Isochrysidales (Groups 1a and 1b subclades included; Richter et al., 2019; Wang et al., 2022) mainly occurs during the spring transitional season. This timing has been shown by seasonal Isochrysidales DNA and alkenone production fluxes in freshwater lakes, including Lake Braya Sø in western Greenland (D'Andrea et al., 2011), Lake Vikvatnet in Norway (D'Andrea et al., 2016), and four lakes (Toolik Lake, Lake E1, E5, and Fog2) in northern Alaska (Longo et al., 2018; Richter et al., 2019). A thermodynamic lake model has demonstrated that the temperatures of surface lake waters at that time in the relatively cold regions respond strongly to winter-spring (or cold-season) air temperature changes (Longo et al., 2020; Richter et al., 2021). Such response is mainly dependent on lake ice thickness in the water and early spring, as well as the timing and duration of spring ice melt (Longo et al., 2020). Colder winter-spring air temperatures could result in thicker lake ice, later ice break-up, and longer duration of spring ice melt, which has a lasting effect on spring lake water temperatures. Throughout the northern mid- and high-latitudes, the U_{37}^{K} values of Group 1 LCAs from surface sediments in freshwater lakes display strong correlation with cold-season temperatures (Longo et al., 2018), showing the potential wide applicability of this proxy in recording this temperature signal. This could fill the important gap in paleoclimate studies as the majority of existing proxies mostly reflect warm season or annual mean temperature signals. Recently, this proxy has been successfully used to reconstruct past winter-spring air temperature changes in Arctic Alaska and Iceland (Longo et al., 2020; Richter et al., 2021).

To further verify the seasonality of Group 1 LCA production in our sediment record, we compare the U_{37}^{K} time series with the instrumental winter-spring and summer temperatures from nearby Arxan weather station (1953–

YAO ET AL. 4 of 10

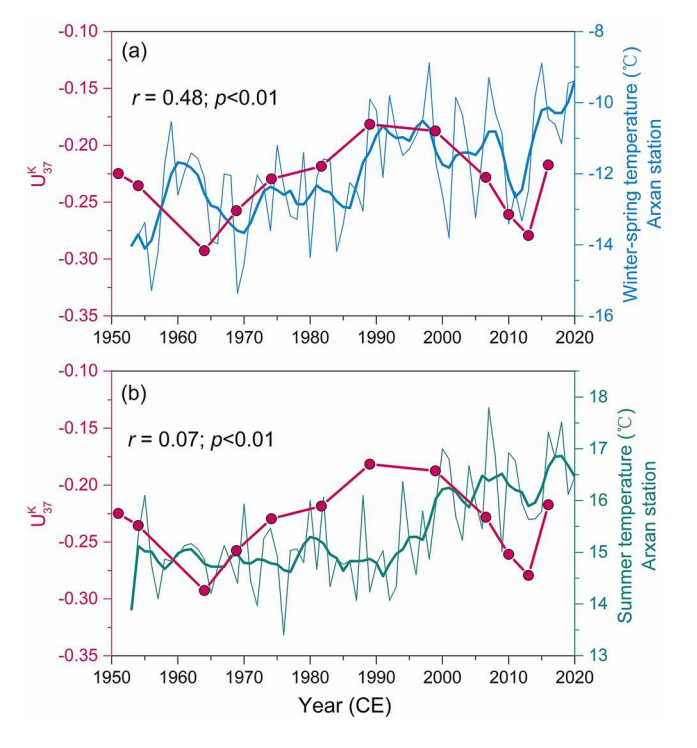


Figure 3. Comparison of the Lake Luming sediment core U_{37}^K time series with the instrumental (a) winter-spring and (b) summer temperatures from the nearby Arxan weather station for the period of 1950–2020 CE. Thick blue lines show 5-point running mean.

2020 CE; Figure 3). The U_{37}^K values are generally consistent with winter-spring temperature (December–May) fluctuations (r=0.48; p<0.01; Figure 3a), but are poorly correlated with summer temperature (June–August) changes (r=0.07; p<0.01; Figure 3b). This analysis reinforces our interpretation that Group 1 LCAs mostly reflect a winter-spring air temperature signal. It is noteworthy that the correlation between U_{37}^K values and winter-spring temperatures is not very strong (r=0.48; p<0.01; Figure 3a). This may be attributed to sediment core dating uncertainties and slightly variable seasonal timing of the highest Group 1 LCA production. Due to the lack of a local specific temperature calibration, we opt not to reconstruct U_{37}^K -inferred absolute temperature variability using our sediment core.

In our entire sediment core, U_{37}^{K} values range from -0.29 to -0.09 (Figure 4a). Before ~ 1830 CE, the U_{37}^{K} values continuously increase, followed by a relatively abrupt decrease until \sim 1880 CE. Afterward, the overall trend of U_{27}^{K} remains almost constant until the present, with relatively low values occurring around 1900, 1964, and 2013 CE. Overall, our record displays relatively high U₃₇^K values during the pre-industrial interval (1750–1850 CE; Figure 4a), indicating cold-season warmth at that time, which is also supported by the relatively high $U_{37}^{K'}$ values (Figure S2b in Supporting Information S1). The warm interval coincides with higher index of extreme warm winter (IEW) values in northeastern China (Chu et al., 2011; Figure 4b). The IEW we compare here is based on descriptions of extreme warm winter events in historical documents (the Annals of the Choson Dynasty; 1392-1910 CE) from the Korean Peninsula (Figure 1a), with higher IEW values indicating warmer winters (Chu et al., 2011). The consistency of our U_{27}^{K} record and the historical data further verifies the reliability of Group 1 LCAs in recording cold-season temperature changes. It is noteworthy that RIK₃₇ values are slightly higher at the interval of 1750-1850 CE, but still generally fall within

the range of Group 1 RIK₃₇ values (Figure 2b). This may be due to potential effect of other environmental factors on the RIK₃₇ of Group 1 alkenones at the relatively warm condition, such as lake trophic status (Longo et al., 2016).

3.3. Driving Mechanisms of Cold-Season Temperature Variability in Northeastern China

The AO and NAO are two prominent modes of large-scale atmospheric circulation variability over the middle and high latitudes of the Northern Hemisphere, especially during the cold season (e.g., Hurrell, 1995; Thompson & Wallace, 1998; Walker, 1928). Numerous observational and modeling studies have demonstrated that the AO and/or NAO significantly affect Eurasian climate at interannual to interdecadal timescales (e.g., reviewed by Bader et al., 2011; He et al., 2017). We compare regional winter-spring temperatures from Arxan station (1953–2020 CE) with annual mean and winter-spring AO and NAO indices (Figure S3 in Supporting Information S1). The winter-spring temperatures are more strongly correlated to the AO index (r = 0.511 for annual mean AO; r = 0.614 for winter-spring AO) relative to the NAO index (r = 0.257 for annual mean NAO; r = 0.399 for winter-spring NAO), especially the winter-spring AO. Therefore, we interpret the AO to be a significant driver of winter-spring temperature variability in our study region.

In our sediment core, the U_{37}^K -inferred cold-season warmth between 1750 and 1850 CE generally corresponds to the period of higher cold-season AO index states, as indicated by more positive January–February coral δ^{18} O values from the northern Red Sea (Felis et al., 2000; Rimbu et al., 2001; Figure 4c). It is noteworthy that AO index in May inferred from oxygen isotope chronologies of larch tree-ring cellulose on the eastern Taimyr Peninsula (Churakova Sidorova et al., 2021) and warm-season AO index inferred from tree-ring width chronologies in Arctic and North Atlantic regions (D'Arrigo et al., 2003) do not display more positive phases between 1750 and 1850 CE (Figure S4 in Supporting Information S1). The disparity of the reconstructed AO could be due to seasonal differentiation of AO variability. Moreover, the NAO did not persistently remain in its positive phase at that time (Trouet et al., 2009; Ortega et al., 2015; Figure 4d). This might be due to the decoupling of the AO and NAO in

YAO ET AL. 5 of 10

1944807, 2023, 10, Downloaded from https://agupubs.oninelibrary.witey.com/doi/10.1029/2023GL103591 by Brown University Library, Witey Online Library on [0309/2023]. See the Terms and Conditions (https://onlinelibrary.witey.com/terms-and-conditions) on Witey Online Library on [0309/2023]. See the Terms and Conditions of the applicable Creative Commons License and Conditions on Witey Online Library for rules of use; OA articles are governed by the applicable Creative Commons License and Conditions on Witey Online Library for rules of use; OA articles are governed by the applicable Creative Commons License and Conditions on Witey Online Library for rules of use; OA articles are governed by the applicable Creative Commons License and Conditions of the Common Conditions of the Conditions of the Common Conditions of the Conditions of

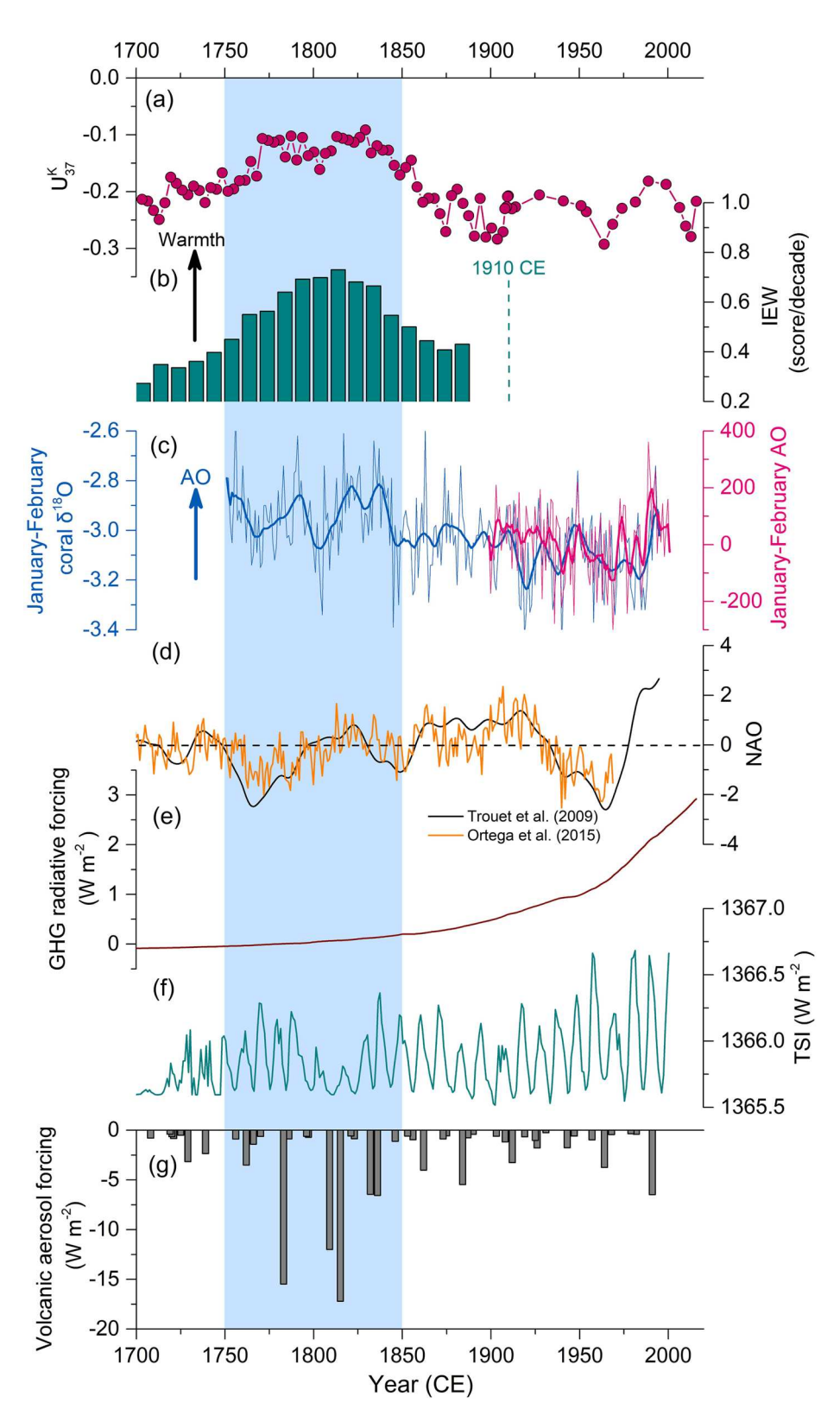


Figure 4.

YAO ET AL. 6 of 10

the cold-season warm climate associated with a different connection to the stratospheric polar vortex anomalies (Hamouda et al., 2021). Thus, the cold-season AO may have played a critical role in driving the cold-season warm climate around 1750–1850 CE. The physical mechanisms may be associated with the strength, frequency, and tracks of cold air and cold surges/cold waves. When the AO is in its positive phase, there is lower-than-normal atmospheric pressure over the polar region and higher-than-normal pressure at the mid-latitudes of the North Pacific and North Atlantic (and vice versa). A stronger westerly jet stream wind stays farther north, reducing cold air outbreaks across the mid-latitudes (e.g., Thompson & Wallace, 1998, 2000). Conversely, the jet stream shifts southward and becomes weaker in the negative AO phase, allowing more frequent penetration of polar cold air outbreaks into the mid-latitudes (e.g., Thompson & Wallace, 1998, 2000). The AO-induced cold anomalies can extend to northeastern China, possibly via the strengthening and southward expansion of the Siberian high that serves as a bridge (He et al., 2017; Jeong & Ho, 2005; Park & Ho, 2011; Woo et al., 2012).

On decadal to multidecadal timescales, solar irradiance and volcanic eruptions are two external forcings affecting temperature variability for the pre-industrial period of the past millennia (e.g., Crowley, 2000; Bauer et al., 2003; PAGES 2k Consortium, 2019). We perform two wavelet coherence analysis to assess the role of TSI and volcanic aerosol forcings on our cold-season temperature record on different timescales (Figure S5 in Supporting Information S1). For the periodicities of ~45–50 years, the U^K₃₇ values show the relatively positive correlation with TSI variability during the period of ~1750–1850 CE (Figure S5a in Supporting Information S1), but have no correlation with volcanic aerosol forcing (Figure S5b in Supporting Information S1). Higher TSI may have led to warmer temperature for the periodicities of ~45–50 years between ~1750 and 1850 CE. At that time, the positive phase of the AO has led to less frequent cold air outbreaks over northeastern China (Figure 4c), so TSI forcing has had additional influence on superimposed multidecadal signals in the cold-season temperature variability. However, when AO was in its negative phase, there were more frequent cold air outbreaks over northeastern China. The influence of TSI on the cold-season temperature variability at the multidecadal timescales may have been counterbalanced or overwhelmed by increased frequency and/or strength of cold air outbreaks induced by the negative AO.

3.4. Implications for Future Cold-Season Temperature Variability

Anthropogenic greenhouse-gas forcing has long been considered the main driver of the accelerated increase of global mean annual temperatures in recent decades (e.g., Stott et al., 2000; Tett et al., 2002). However, this driver clearly does not explain the weak trend or even cooling of cold seasons observed in northern mid-latitude continents at the same timescale (e.g., J. Cohen et al., 2020; J. L.Cohen et al., 2012; McCusker et al., 2016; Mori et al., 2019). In our sediment core, we extend the cold-season temperature record of northeastern China beyond the industrial revolution, providing a longer-term perspective for recent climatic anomalies. Our record shows an overall colder cold-season climate since the industrial revolution (1850 CE) relative to the pre-industrial period of 1700–1850 CE (Figure 4a), which does not directly correspond to the strong increases of anthropogenic greenhouse-gas radiative forcing (Figure 4e). Rather, our analyses have suggested that this temperature variability is a direct response to internal cold-season AO forcing. However, it is possible that rising greenhouse gases have indirectly impacted the AO variability.

AO variability in the future could help predict the frequency of extreme cold events over northeastern China and other AO-affected mid-latitude regions. Some model and observational studies have shown a possible linkage between the Arctic sea-ice loss and negative AO phase in recent decades (e.g., Honda et al., 2009; Kim et al., 2014; Liu et al., 2012; Mori et al., 2019; Wu & Zhang, 2010). If this is true, more frequent cold extremes would be expected to occur in AO-affected mid-latitude regions in response to future reductions of Arctic sea ice with global warming.

4. Conclusions

In this study, we take advantage of high sediment accumulation rates in Lake Luming in northeastern China to verify the reliable application of the Group 1 alkenone U_{37}^K proxy for past cold-season temperature reconstruction

Figure 4. Group 1 U_{37}^K -inferred cold-season temperature variations and climate forcings for the period of 1700–2020 CE. (a) The U_{37}^K values in the Lake Luming sediment core (this study). (b) Index of extreme warm winter events in northeastern China based on descriptions in historical documents (the Annals of the Choson Dynasty; 1392–1910 CE) on the Korean Peninsula (Chu et al., 2011; 3-point running mean). (c) January–February Ras Umm Sidd coral δ^{18} O values from the northern Red Sea (Felis et al., 2000; Rimbu et al., 2001; blue thick line shows 10-point running mean) and Arctic Oscillation data between 1899 and 2002 (research.jisao. washington.edu/data_sets/aots/; the time series has not been standardized; red thick line shows 5-point running mean). (d) North Atlantic Oscillation index (Ortega et al., 2015; Trouet et al., 2009). (e) Radiative forcing due to atmospheric greenhouse gases including CO_2 , CH_4 , and NO_2 (Köhler et al., 2017). (f) Total solar irradiance (Lean, 2000). (g) Global volcanic aerosol forcing (Sigl et al., 2015). Blue shading notes the period of the 1750–1850 CE.

YAO ET AL. 7 of 10

19448007, 2023, 10, Downlo

by comparing with instrumental and historical records in the region. Our unique alkenone record spans past 300 years and indicates warmer cold-season conditions during the pre-industrial era (1750-1850 CE) relative to the anthropogenic industrial period (since 1850 CE). This warmth can be largely attributed to more positive cold-season AO states, which may reduce cold air outbreaks over northeastern China. In the future, a more causative understanding of the linkages between AO and Arctic climate (such as sea ice loss) would help uncover the predictability of cold-season temperature variability in mid-latitude regions.

Data Availability Statement

The research data used in this study are submitted to the datasets of 4TU. Research Date, which is available at https://doi.org/10.4121/21789452.v2.

Acknowledgments

This work was supported by the National Natural Science Foundation of China (Nos. 42073070; 42130503; 41888101). We thank Dr. J. Zhao and J. Jing for assistance during field sampling, and Dr H. Li for discussions. We are also grateful for the comments from three anonymous reviewers and editor Dr. Sarah Feakins that helped us improve the manuscript.

References

- Appleby, P. G. (2002). Chronostratigraphic techniques in recent sediments. In Tracking environmental change using lake sediments (pp. 171-203).
- Bader, J., Mesquita, M. D. S., Hodges, K. I., Keenlyside, N., Østerhus, S., & Miles, M. (2011). A review on Northern Hemisphere sea-ice. storminess and the North Atlantic Oscillation: Observations and projected changes. Atmospheric Research, 101(4), 809-834. https://doi. org/10.1016/i.atmosres.2011.04.007
- Baker, J. L., Lachniet, M. S., Chervyatsova, O., Asmerom, Y., & Polyak, V. J. (2017). Holocene warming in western continental Eurasia driven by glacial retreat and greenhouse forcing. Nature Geoscience, 10(6), 430-435. https://doi.org/10.1038/ngeo2953
- Bauer, E., Claussen, M., Brovkin, V., & Huenerbein, A. (2003). Assessing climate forcings of the Earth system for the past millennium. Geophysical Research Letters, 30(6), 1276. https://doi.org/10.1029/2002g1016639
- Brassell, S. C., Eglinton, G., Marlowe, I. T., Pflaumann, U., & Sarnthein, M. (1986). Molecular stratigraphy: A new tool for climatic assessment. Nature, 320(6058), 129-133. https://doi.org/10.1038/320129a0
- Chu, G., Sun, Q., Wang, X., Liu, M., Lin, Y., Xie, M., et al. (2011). Seasonal temperature variability during the past 1600 years recorded in historical documents and varved lake sediment profiles from northeastern China. The Holocene, 22(7), 785-792. https://doi. org/10.1177/0959683611430413
- Churakova Sidorova, O. V., Siegwolf, R. T. W., Fonti, M. V., Vaganov, E. A., & Saurer, M. (2021). Spring arctic oscillation as a trigger of summer drought in Siberian subarctic over the past 1494 years. Scientific Reports, 11(1), 19010. https://doi.org/10.1038/s41598-021-97911-2
- Cohen, J., Zhang, X., Francis, J., Jung, T., Kwok, R., Overland, J., et al. (2020). Divergent consensuses on Arctic amplification influence on midlatitude severe winter weather. Nature Climate Change, 10(1), 20-29. https://doi.org/10.1038/s41558-019-0662-y
- Cohen, J. L., Furtado, J. C., Barlow, M. A., Alexeev, V. A., & Cherry, J. E. (2012). Asymmetric seasonal temperature trends. Geophysical Research Letters, 39(4), L04705. https://doi.org/10.1029/2011gl050582
- Crowley, T. J. (2000). Causes of climate change over the past 1000 years. Science, 289(5477), 270-277. https://doi.org/10.1126/ science.289.5477.270
- D'Andrea, W. J., Huang, Y., Fritz, S. C., & Anderson, N. J. (2011). Abrupt Holocene climate change as an important factor for human migration in West Greenland. Proceedings of the National Academy of Sciences of the United States of America, 108(24), 9765–9769. https://doi.
- D'Andrea, W. J., Theroux, S., Bradley, E. S., & Huang, X. (2016). Does phylogeny control U₃₇^K-temperature sensitivity? Implications for lacustrine alkenone paleothermometry. Geochimica et Cosmochimica Acta, 175, 168-180. https://doi.org/10.1016/j.gca.2015.10.031
- D'Arrigo, R. D., Cook, E. R., Mann, M. E., & Jacoby, G. C. (2003). Tree-ring reconstructions of temperature and sea-level pressure variability associated with the warm-season Arctic Oscillation since AD 1650. Geophysical Research Letters, 30(11), 1549. https://doi.
- Emile-Geay, J., McKay, N. P., Kaufman, D. S., von Gunten, L., Wang, J., Anchukaitis, K. J., et al. (2017). A global multiproxy database for temperature reconstructions of the Common Era. Scientific Data, 4(1), 170088. https://doi.org/10.1038/sdata.2017.88
- Felis, T., Pätzold, J., Loya, Y., Fine, M., Nawar, A. H., & Wefer, G. (2000). A coral oxygen isotope record from the northern Red Sea documenting NAO, ENSO, and North Pacific teleconnections on Middle East climate variability since the year 1750. Paleoceanography, 15(6), 679-694. https://doi.org/10.1029/1999pa000477
- Grinsted, A., Moore, J. C., & Jevrejeva, S. (2004). Application of the cross wavelet transform and wavelet coherence to geophysical time series. Nonlinear Processes in Geophysics, 11(5/6), 561-566. https://doi.org/10.5194/npg-11-561-2004
- Hamouda, M. E., Pasquero, C., & Tziperman, E. (2021). Decoupling of the Arctic Oscillation and North Atlantic Oscillation in a warmer climate. Nature Climate Change, 11(2), 137-142. https://doi.org/10.1038/s41558-020-00966-8
- He, S., Gao, Y., Li, F., Wang, H., & He, Y. (2017). Impact of Arctic Oscillation on the East Asian climate: A review. Earth-Science Reviews, 164, 48-62. https://doi.org/10.1016/j.earscirev.2016.10.014
- Holland, K. M., Porter, T. J., Froese, D. G., Kokelj, S. V., & Buchanan, C. A. (2020). Ice-wedge evidence of Holocene winter warming in the Canadian Arctic. Geophysical Research Letters, 47(12), e2020GL087942. https://doi.org/10.1029/2020gl087942
- Honda, M., Inoue, J., & Yamane, S. (2009). Influence of low Arctic sea-ice minima on anomalously cold Eurasian winters. Geophysical Research Letters, 36(8), L08707, https://doi.org/10.1029/2008g1037079
- Hurrell, J. W. (1995). Decadal trends in the North Atlantic Oscillation: Regional temperatures and precipitation. Science, 269(5224), 676-679. https://doi.org/10.1126/science.269.5224.676
- Jeong, J.-H., & Ho, C.-H. (2005). Changes in occurrence of cold surges over east Asia in association with Arctic Oscillation. Geophysical Research Letters, 32(14), L14704. https://doi.org/10.1029/2005gl023024
- Kim, B.-M., Son, S.-W., Min, S.-K., Jeong, J.-H., Kim, S.-J., Zhang, X., et al. (2014). Weakening of the stratospheric polar vortex by Arctic sea-ice loss. Nature Communications, 5(1), 4646. https://doi.org/10.1038/ncomms5646
- Köhler, P., Nehrbass-Ahles, C., Schmitt, J., Stocker, T. F., & Fischer, H. (2017). Compilations and splined-smoothed calculations of continuous records of the atmospheric greenhouse gases CO2, CH4, and N2O and their radiative forcing since the penultimate glacial maximum. Earth System Science Data, 9(1), 363-387. https://doi.org/10.5194/essd-9-363-2017

YAO ET AL. 8 of 10

- Lean, J. (2000). Evolution of the Sun's spectral irradiance since the Maunder Minimum. Geophysical Research Letters, 27(16), 2425–2428. https://doi.org/10.1029/2000g1000043
- Liu, J., Curry, J. A., Wang, H., Song, M., & Horton, R. M. (2012). Impact of declining Arctic sea ice on winter snowfall. Proceedings of the National Academy of Sciences, 109(11), 4074–4079. https://doi.org/10.1073/pnas.1114910109
- Longo, W. M., Dillon, J. T., Tarozo, R., Salacup, J. M., & Huang, Y. (2013). Unprecedented separation of long chain alkenones from gas chromatography with a poly(trifluoropropylmethylsiloxane) stationary phase. *Organic Geochemistry*, 65, 94–102. https://doi.org/10.1016/j.orgeochem.2013.10.011
- Longo, W. M., Huang, Y., Russell, J. M., Morrill, C., Daniels, W. C., Giblin, A. E., & Crowther, J. (2020). Insolation and greenhouse gases drove Holocene winter and spring warming in Arctic Alaska. *Quaternary Science Reviews*, 242, 106438. https://doi.org/10.1016/j. quascirev.2020.106438
- Longo, W. M., Huang, Y., Yao, Y., Zhao, J., Giblin, A. E., Wang, X., et al. (2018). Widespread occurrence of distinct alkenones from Group I haptophytes in freshwater lakes: Implications for paleotemperature and paleoenvironmental reconstructions. *Earth and Planetary Science Letters*, 492, 239–250. https://doi.org/10.1016/j.epsl.2018.04.002
- Longo, W. M., Theroux, S., Gibin, A. E., Zheng, Y., Dillon, J. T., & Huang, Y. (2016). Temperature calibration and phylogenetically distinct distributions for freshwater alkenones: Evidence from northern Alaskan lakes. *Geochimica et Cosmochimica Acta*, 180, 177–196. https://doi. org/10.1016/j.gca.2016.02.019
- Lu, J., Yao, Y., Zhu, Z., Sun, C., Wu, J., & Liu, J. (2021). Relationship between brGDGT-based temperatures and volcanism record in the recent 300 years in Arxan region. *Quaternary Sciences*, 41, 88–98.
- McCusker, K. E., Fyfe, J. C., & Sigmond, M. (2016). Twenty-five winter of unexpected Eurasian cooling unlikely due to Arctic sea-ice loss. Nature Geoscience, 9(11), 838–842. https://doi.org/10.1038/ngeo2820
- Meyer, H., Opel, T., Laepple, T., Dereviagin, A. Y., Hoffmann, K., & Werner, M. (2015). Long-term winter warming trend in the Siberian Arctic during the mid-to late Holocene. *Nature Geoscience*, 8(2), 122–125. https://doi.org/10.1038/ngeo2349
- Mori, M., Kosaka, Y., Watanabe, M., Nakamura, H., & Kimoto, M. (2019). A reconciled estimate of the influence of Arctic sea-ice loss on recent Eurasian cooling. *Nature Climate Change*, 9(2), 123–129. https://doi.org/10.1038/s41558-018-0379-3
- Novak, J., McGrath, S. M., Wang, K. J., Liao, S., Clemens, S. C., Kuhnt, W., & Huang, Y. (2022). U38MEK' Expands the linear dynamic range of the alkenone sea surface temperature proxy. *Geochimica et Cosmochimica Acta*, 328, 207–220. https://doi.org/10.1016/j.gca.2022.04.021
- Ortega, P., Lehner, F., Swingedouw, D., Masson-Delmotte, V., Raible, C. C., Casado, M., & Yiou, P. (2015). A model-tested North Atlantic Oscillation reconstruction for the past millennium. *Nature*, 523(7558), 71–74. https://doi.org/10.1038/nature14518
- Overland, J. E., Wood, K. R., & Wang, M. (2011). Warm Arctic-cold continents: Climate impacts of the newly open Arctic sea. *Polar Research*,
- 30(1), 15787. https://doi.org/10.3402/polar.v30i0.15787
 PAGES 2k Consortium. (2019). Consistent multidecadal variability in global temperature reconstructions and simulations over the Common Era.
- Nature Geoscience, 12(8), 643–649. https://doi.org/10.1038/s41561-019-0400-0
 Park, T.-W., Ho, C.-H., & Yang, S. (2011). Relationship between the Arctic Oscillation and cold surges over East Asia. Journal of Climate, 24(1),
- 68–83. https://doi.org/10.1175/2010jcli3529.1
- Pithan, F., & Mauritsen, T. (2014). Arctic amplification dominated by temperature feedbacks in contemporary climate models. *Nature Geoscience*, 7(3), 181–184. https://doi.org/10.1038/ngeo2071
- Prahl, F. G., & Wakeham, S. G. (1987). Calibration of unsaturation patterns in long-chain ketone compositions for palaeotemperature assessment. Nature, 330(6146), 367–369. https://doi.org/10.1038/330367a0
- Rao, Z., Shi, F., Li, Y., Huang, C., Zhang, X., Yang, W., et al. (2020). Long-term winter/summer warming trends during the Holocene revealed by α-cellulose δ¹⁸O/δ¹³C records from an alpine peat core from central Asia. *Quaternary Science Reviews*, 232, 106217. https://doi.org/10.1016/j.quascirev.2020.106217
- Richter, N., Longo, W. M., George, S., Shipunova, A., Huang, Y., & Amaral-Zettler, L. (2019). Phylogenetic diversity in freshwater-dwelling Isochrysidales haptophytes with implications for alkenone production. *Geobiology*, 17(3), 272–280. https://doi.org/10.1111/gbi.12330
- Richter, N., Russell, J. M., Garfinkel, J., & Huang, Y. (2021). Winter-spring warming in the North Atlantic during the last 2000 years: Evidence from southwest Iceland. Climate of the Past, 17(3), 1363–1383. https://doi.org/10.5194/cp-17-1363-2021
- Rimbu, N., Lohmann, G., Felis, T., & Pätzold, J. (2001). Arctic Oscillation signature in a Red Sea coral. *Geophysical Research Letters*, 28(15), 2959–2962. https://doi.org/10.1029/2001g1013083
- Sanchez-Cabeza, J. A., & Ruiz-Fernández, A. C. (2012). ²¹⁰Pb sediment radiochronology: An integrated formulation and classification of dating models. *Geochimica et Cosmochimica Acta*, 82, 183–200. https://doi.org/10.1016/j.gca.2010.12.024
- Sigl, M., Winstrup, M., McConnell, J. R., Welten, K. C., Plunkett, G., Ludlow, F., et al. (2015). Timing and climate forcing of volcanic eruptions for the past 2.500 years. *Nature*. 523(7562), 543–549. https://doi.org/10.1038/nature14565
- Stocker, T. F., Qin, D., Plattner, G. K., Tignor, M., Allen, S. K., Boschung, J., et al. (2013). Climate change: The physical science basis. Contribution of Working Group 1 to the fifth assessment report of the intergovernmental panel on climate change (pp. 383–464). Cambridge University Press.
- Stott, P. A., Tett, S. F. B., Jones, G. S., Allen, M. R., Mitchell, J. F. B., & Jenkins, G. J. (2000). External control of 20th century temperature by natural and anthropogenic forcings. *Science*, 290(5499), 2133–2137. https://doi.org/10.1126/science.290.5499.2133
- Tett, S. F. B., Jones, G. S., Stott, P. A., Hill, D. C., Mitchell, J. F. B., Allen, M. R., et al. (2002). Estimation of natural and anthropogenic contributions to twentieth century temperature change. *Journal of Geophysical Research*, 107, ACL 10-1–ACL 10-24.
- Theroux, S., D'Andrea, W. J., Toney, J., Amaral-Zettler, L., & Huang, Y. (2010). Phylogenetic diversity and evolutionary relatedness of alkenone-producing haptophyte algae in lakes: Implications for continental paleotemperature reconstructions. *Earth and Planetary Science Letters*, 300(3–4), 311–320. https://doi.org/10.1016/j.epsl.2010.10.009
- Thompson, D. W. J., & Wallace, J. M. (1998). The Arctic oscillation signature in the wintertime geopotential height and temperature fields. Geophysical Research Letters, 25(9), 1297–1300. https://doi.org/10.1029/98gl00950
- Thompson, D. W. J., & Wallace, J. M. (2000). Annular modes in the extratropical circulation. Part I: Month-to-month variability. *Journal of Climate*, 13(5), 1000–1016. https://doi.org/10.1175/1520-0442(2000)013<1000:amitec>2.0.co;2
- Torrence, C., & Compo, G. P. (1998). A practical guide to wavelet analysis. Bulletin of the American Meteorological Society, 79(1), 61–78. https://doi.org/10.1175/1520-0477(1998)079<0061:apgtwa>2.0.co;2
- Trouet, V., Esper, J., Graham, N. E., Baker, A., Scourse, J. D., & Frank, D. C. (2009). Persistent positive North Atlantic Oscillation mode dominated the Medieval Climate Anomaly. Science, 324(5923), 78–80. https://doi.org/10.1126/science.1166349
- Walker, G. (1928). World weather. Monthly Weather Review, 56(5), 167-170. https://doi.org/10.1175/1520-0493(1928)56<167:ww>2.0.co;2
- Wang, L., Tian, M., Wen, X., Zhao, L., Song, J., Sun, M., et al. (2014). Geoconservation and geotourism in Arxan-Chaine Colcanic Area, Inner Mongolia, China. Quaternary International, 349, 384–391. https://doi.org/10.1016/j.quaint.2014.06.024

YAO ET AL. 9 of 10

- Wang, L., Yao, Y., Huang, Y., Cai, Y., & Cheng, H. (2022). Group 1 phylogeny and alkenone distributions in a freshwater volcanic lake of northeastern China: Implications for paleotemperature reconstructions. Organic Geochemistry, 172, 104483. https://doi.org/10.1016/j. orggeochem.2022.104483
- Woo, S.-H., Kim, B.-M., Jeong, J.-H., Kim, S.-J., & Lim, G.-H. (2012). Decadal changes in surface air temperature variability and cold surge characteristics over northeast Asia and their relation with the Arctic Oscillation for the past three decades (1979–2011). *Journal of Geophysical Research*, 117(D18), D18117. https://doi.org/10.1029/2011jd016929
- Wu, Q., & Zhang, X. (2010). Observed forcing-feedback processes between Northern Hemisphere atmospheric circulation and Arctic sea ice coverage. Journal of Geophysical Research, 115(D14), D14119. https://doi.org/10.1029/2009jd013574
- Yao, Y., Lan, J., Zhao, J., Vachula, R. S., Xu, H., Cai, Y., et al. (2020). Abrupt freshening since the early Little Ice Age in Lake Sayram of arid central Asia inferred from an alkenone isomer proxy. *Geophysical Research Letters*, 47(16), e2020GL089257. https://doi.org/10.1029/2020gl089257
- Yao, Y., Zhao, J., Longo, W. M., Li, G., Wang, X., Vachula, R. S., et al. (2019). New insights into environmental controls on the occurrence and abundance of Group I alkenones and their paleoclimate applications: Evidence from volcanic lakes of northeastern China. Earth and Planetary Science Letters, 527, 115792. https://doi.org/10.1016/j.epsl.2019.115792
- Yao, Y., Zhao, J., Vachula, R. S., Liao, S., Li, G., Pearson, E. J., & Huang, Y. (2022). Phylogeny, alkenone profiles and ecology of Isochrysidales subclades in saline lakes: Implications for paleosalinity and paleotemperature reconstructions. *Geochimica et Cosmochimica Acta*, 317, 472–487. https://doi.org/10.1016/j.gca.2021.11.001
- Zheng, Y., Tarozo, R., & Huang, Y. (2017). Optimizing chromatographic resolution for simultaneous quantification of long chain alkenones, alkenoates and their double bond positional isomers. *Organic Geochemistry*, 111, 136–143. https://doi.org/10.1016/j.orggeochem.2017.06.013

YAO ET AL. 10 of 10